

Temporally Identity-Aware SSD with Attentional LSTM

Xingyu Chen, Junzhi Yu, *Senior Member, IEEE*, and Zhengxing Wu

Abstract—Temporal object detection has attracted significant attention, but most popular detection methods can not leverage the rich temporal information in videos. Very recently, many different algorithms have been developed for video detection task, but real-time online approaches are frequently deficient. In this paper, based on attention mechanism and convolutional long short-term memory (ConvLSTM), we propose a temporal signal-shot detector (TSSD) for real-world detection. Distinct from previous methods, we take aim at temporally integrating pyramidal feature hierarchy using ConvLSTM, and design a novel structure including a low-level temporal unit as well as a high-level one (HL-TU) for multi-scale feature maps. Moreover, we develop a creative temporal analysis unit, namely, attentional ConvLSTM (AC-LSTM), in which a temporal attention module is specially tailored for background suppression and scale suppression while a ConvLSTM integrates attention-aware features through time. An association loss is designed for temporal coherence. Besides, online tubelet analysis (OTA) is exploited for identification. Finally, our method is evaluated on ImageNet VID dataset and 2DMOT15 dataset. Extensive comparisons on the detection and tracking capability validate the superiority of the proposed approach. Consequently, the developed TSSD-OTA is fairly faster and achieves an overall competitive performance in terms of detection and tracking. The source code will be made available.

Index Terms—Object detection, Tracking by detection, Video processing, Sequential learning.

I. INTRODUCTION

Taking advantage of the convolutional neural network (CNN), existing detection methods fall into two categories, i.e., one-stage and two-stage detectors. The former is represented by RCNN family [1]–[4], RFCN [5], and FPN [6], all of which detect objects based on region proposal. On the other hand, YOLO [7], SSD [8], RetinaNet [9], and etc., treat the localization task as a regression, where the regression and classification can be computed simultaneously with signal-shot multi-box algorithms. In particular, making use of CNN’s features more effectively, SSD is one of the first methods that adopt the pyramidal feature hierarchy for detection. However, most works have largely focused on detecting in static images, ignoring temporal consistency in videos. Thus, it is imperative to develop an approach to integrate spatial features with

temporal information. In addition, considering the trade-off between detection speed and accuracy, the one-stage detector is more suitable for real-world applications in terms of current research status.

Recurrent neural network (RNN) has achieved great success in some sequence processing tasks [10], [11]. Typically, long short-term memory (LSTM) is proposed for longer sequence learning [12]. For spatiotemporal visual features, Shi et al. developed convolutional LSTM (ConvLSTM) to associate LSTM with spatial structure [13]. However, as for detection, selecting discriminative features for ConvLSTM is a pivotal step, because only a small part of visual features can devote themselves to detecting. Fortunately, attention is an exciting idea which imitates human’s cognitive patterns, promoting CNN concern on essential information. For example, Mnih et al. proposed a recurrent attention model (RAM) to find the most suitable local feature for image classification [15]. Yet, attention-based temporal model for image-sequence detection has been relatively deficient.

As a closely relevant field, object tracking requires the initial position to be known a priori [36]. Moreover, detection and tracking are moving towards unity in recent years, where a detector and a tracker tend to be cascaded in most up-to-date approaches [22], [46]. This solution generally raises model complexity and computational cost. Hence, it is worthwhile to exploit a tracker-like detector for their in-depth combination and time efficiency. Tracking by detection is a popular idea, advocating that a detector should output tracker-like results, where the tracking component is actually designed for data association [23], [24], [45], [47]. Nevertheless, the detector and tracking component are usually independent in existing tracking by detection framework, so it is essential to jointly investigate their performance.

In this paper, we jointly design a identity-aware detector. Taking aim at detecting objects in temporally coherent vision, we propose a temporal detection model based on SSD, namely, temporal single-shot detector (TSSD). To integrate features through time, ConvLSTMs are employed for temporal information. Due to the pyramidal feature hierarchy for multi-scale detection, the SSD always generates a large body of visual features with multi-scale semantic information, thus we design a new structure including a low-level temporal unit as well as a high-level one (HL-TU) for their temporal propagation. Furthermore, as for multi-scale feature maps, only a small part of visual features are related to objects. Thereby, attention mechanism is adopted for background suppression and scale suppression, then we propose an attentional ConvLSTM (AC-LSTM) module. Subsequently, an association objective is de-

This work was supported by the National Natural Science Foundation of China (nos. 61633004, 61633020, 61603388, and 61633017), and by the Beijing Natural Science Foundation (nos. 4164103 and 4161002).

X. Chen is with the University of Chinese Academy of Sciences, Beijing 100049, China, chenxingyu2015@ia.ac.cn

X. Chen, J. Yu, and Z. Wu are with the State Key Laboratory of Management and Control for Complex Systems, Institute of Automation, Chinese Academy of Sciences, Beijing 100190, China, {chenxingyu2015, junzhi.yu, zhengxing.wu}@ia.ac.cn

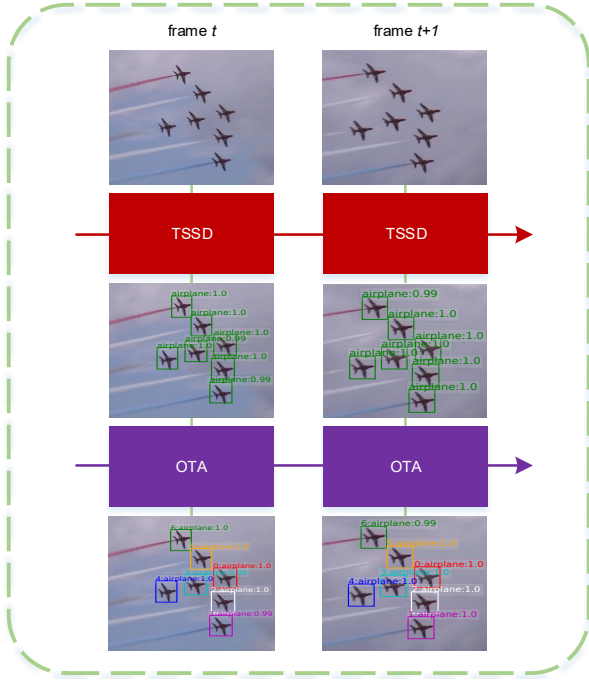


Fig. 1. We aim to do temporally detect objects in video, and generate tracking-like results with low computational costs. The TSSD is a temporal detector, and the OTA is designed for identification.

veloped for sequence training. Finally, online tubelet analysis (OTA) will be carried out for identification. As a consequence, the TSSD-OTA achieves considerable detection and tracking performance for consecutive vision in terms of both precision and speed. Our proposed pipeline is schematically shown in Fig. 1. To the best of our knowledge, only few temporal one-stage detectors have been reported. Moreover, a real-time, online, and identify-aware detector is absent in existing detection frameworks. The contributions made in this paper are summarized as follows:

- We design an HL-TU structure to effectively propagate pyramidal feature hierarchy through time. Moreover, We propose an AC-LSTM module as a temporal analysis unit, in which useless information is reduced.
- An association loss function and training tricks are developed for temporal coherence. Specifically, our association loss does not require any extra ground truth labels (e.g., identity label).
- For identification, an OTA algorithm is exploited with low-level AC-LSTM, which can be treated as a siamese network [42] through time.
- We achieve a considerably improved results on ImageNet VID dataset and 2DMOT15 dataset in terms of detection and tracking.

II. RELATED WORK

A. Post-Processing Method

At the beginning, static detection and post-proposing methods are combined to counteract video detection task [16]–[18]. They statically detect in each video frame, and then,

comprehensively deal with multi-frame results. Kang et al. developed detection methods based on tubelet, which is defined as temporally propagative bounding boxes in video snippet [16], [17]. Their method TCNN contains still-image object detection, multi-context suppression, motion guided propagation, and temporal tubelet re-scoring. Taking inspire from non-maximum suppression (NMS), Han et al. proposed SeqNMS to suppress temporally discontinuous bounding boxes. However, these solutions come with two major drawbacks. Firstly, due to complex post-processing, the time efficiency may decrease. On the other hand, such methods do not improve the performance of the detector itself.

B. Detection Based on Region Proposal

Faster RCNN uses region proposal network for object localization [3], so some approaches for video detection try to enhance the effectiveness of RPN with temporal information [19]–[21], [27], [38]. Galteri et al. designed a closed-loop RPN to merge new proposals with previous detection results. This method effectively reduces the number of invalid regions, but it may also make the proposed regions excessively concentrated. Kang et al. developed tubelet proposal networks (TPN) to generate tubelets rather than bounding boxes. Then, an encoder-decoder LSTM is used for classification. TPN integrates temporal information, but it requires the future messages. Such methods are extended from two-stage detectors, so they usually suffer the problem with time efficiency.

C. Detection and Tracking

Feichtenhofer et al. associated a RFCN detector with a correlation-filter-based tracker [36] to detect objects in videos, called D&T [22]. Thanks to tracking method, they achieve a high recall rate, but obviously, this cascaded system could seriously increase the model complexity, hence they can hardly work in real time, especially when a large number of objects appear in a video snippet.

In terms of tracking by detection, Xiang et al. converted the tracking task to decision making, and their policy relies on tracking states [45]. H. Kim and C. Kim combined a detector, a forward tracker, and a backward tracker for tracing multiple objects in video sequences, and the detector was also used to refine tracking results [46]. Ning et al. proposed ROLO based on YOLO and LSTM for tracking [23]. The YOLO is responsible for static detection, and the visual features as well as positions of high-score objects will be fed to LSTM for temporally modeling. Lu et al. proposed association LSTM (ALSTM) for to temporally analyze relations of high-score objects, and an association loss was designed for identification [24]. Pragmatically, Bewley et al. developed SORT with Kalman filter [49] and Hungarian method [50] for real-time tracking [47], and the tracking component achieves a speed of 260 frames per second (FPS). Obviously, only detection results build connection between a detector and a tracker in these frameworks.

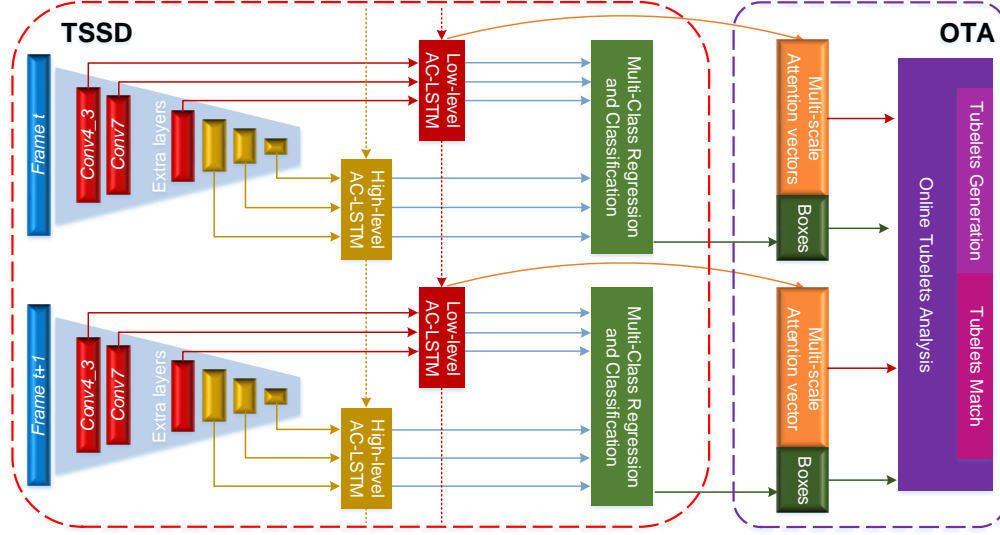


Fig. 2. Schematic illustration of the TSSD-OTA. The high-level features share an AC-LSTM and low-level features do so, namely, HL-TU. Next, the hidden states of ConvLSTM will be used for multi-box regression and classification. Eventually, based on multi-scale attention maps, online tubelet analysis is conducted for identification. This figure is best viewed in color.

D. RNN-Based Detector

Very recently, Up-to-date approaches have associated the detector with RNN. Liu and Zhu reported a mobile video detection method based on SSD and LSTM, called LSTM-SSD [28]. Moreover, they also designed a Bottleneck-LSTM structure to reduce computational costs. As a result, LSTM-SSD reached a real-time inference speed of up to 15 FPS on a mobile CPU. Xiao and Lee developed a spatial-temporal memory module (STMM) with ConvGRU [14] for temporal information propagation [27]. In particular, “MatchTrans” was proposed to suppress the redundant memory.

III. APPROACH

In this section, we firstly present the proposed architecture, including HL-TU and AC-LSTM. Then, we describe how to train the network in detail. Finally, the methodologies of OTA algorithm will be briefed.

A. Architecture

Extending from SSD with VGG-16 [25] as the backbone, we build a temporal architecture, where $fc6, fc7$ in original VGG-16 are converted to convolutional layers, namely, $Conv6, Conv7$. Referring to the Fig. 2, the proposed TSSD is based on forward CNN and RNN that generates a fixed number of bounding boxes and the category-discriminative scores indicating the presence different classes of objects on those boxes, followed the NMS to generate the final results. The spatial resolution of the input image is 300×300 . $Conv4_3, Conv7, Conv8_2, Conv9_2, Conv10_2, Conv11_2$ are employed as pyramidal features, whose size are $38 \times 38 \times 512, 19 \times 19 \times 512, 10 \times 10 \times 512, 5 \times 5 \times 256, 3 \times 3 \times 256$, and $1 \times 1 \times 256$, respectively. As for sequence

learning, the TSSD is equipped with multi-scale feature-integration structures, i.e. HL-TU and AC-LSTM. The HL-TU takes aim at propagation of pyramidal feature hierarchy, whereas AC-LSTM aims to effectively produce temporal memory without useless information.

1) *HL-TU*: We use the same two structures to integrate the pyramidal feature hierarchy temporally, called HL-TU. There are pyramidal features for six-scale semantic information in adopted SSD model, and their feature sizes are diverse from each other. In original SSD framework, there are 512, 1024, 512, 256, 256, 256 channels in features from low-level to high-level. Creatively, we divide the multi-scale feature maps into two categories according to their hierarchical relation and channel sizes, i.e., low-level features and high-level features. Therefore, as illustrated in Fig. 2, we treat the first three feature maps as low-level features (shown in red), whereas the last three maps are considered as high-level features (shown in gold). The channel numbers of low-level features are unified as 512 to share a temporal unit while that of high-level features remain as 256. Additionally, the low-level features cover more details, whereas the high-level features contain more semantic information. Correspondingly, the HL-TU including a low-level temporal unit and a high-level one is designed for them.

2) *AC-LSTM*: In object detection task, most features are related to background. Moreover, feature maps in different scales contribute to detection in different degrees. Therefore, it is inefficient when a ConvLSTM handles background or aforementioned small-contributed multi-scale feature maps. For example, if an object’s size is too small, its detection will be contributed by $Conv4_3$, in which features associated with the small object are far less than that for background. Moreover, all the higher-level feature maps can be considered useless, which should be suppressed to avoid the false positive. To that

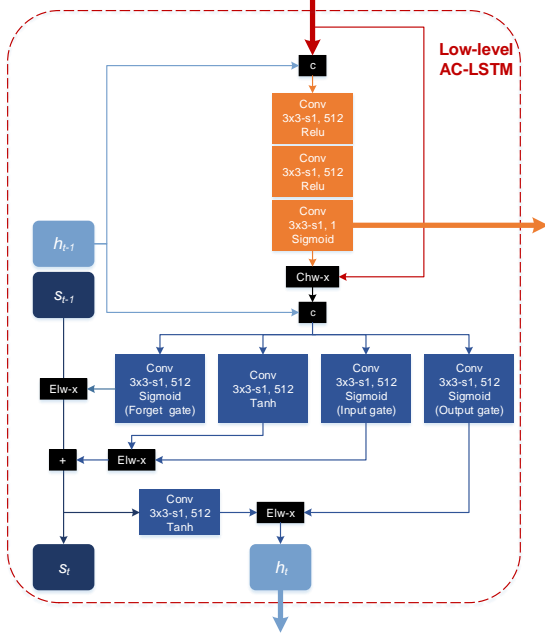


Fig. 3. Implementation detail of AC-LSTM. “c” denotes concatenation; “Chw-x”, “Elw-x” represent channel-wise and element-wise multiplication, respectively; “+” is element-wise summation.

end, we propose an AC-LSTM for background suppression and scale suppression, in which a temporal attention module selects object-aware features for a ConvLSTM, and in turn, the ConvLSTM provides the attention module with temporal information to improve attention accuracy. As a temporal analysis unit, AC-LSTM can be formulated as follows,

$$\begin{aligned}
 a_t &= \sigma(W_a * [x, h_{t-1}]) \\
 i_t &= \sigma(W_i * [a_t \circ x, h_{t-1}] + b_i) \\
 f_t &= \sigma(W_f * [a_t \circ x, h_{t-1}] + b_f) \\
 o_t &= \sigma(W_o * [a_t \circ x, h_{t-1}] + b_o) \\
 c_t &= \tanh(W_c * [a_t \circ x, h_{t-1}] + b_c) \\
 s_t &= (f_t \odot s_{t-1}) + (i_t \odot c_t) \\
 h_t &= o_t \odot \tanh(s_t),
 \end{aligned} \tag{1}$$

where $*$ denotes convolution operation; $[\cdot, \cdot]$ is concatenation; \odot is element-wise multiplication; and \circ represents that a one-channel map multiplies with each channel in a multi-channel feature map. At time step t , $a_t, h_t, i_t, f_t, o_t, c_t, s_t$ are attention map, hidden state, input gate, forget gate, output gate, LSTM’s incoming information and memory, respectively. σ represents sigmoid activation function.

As shown in Fig. 3, the AC-LSTM is designed with CNN and RNN. Current feature map (x) and previous hidden state (h_{t-1}) serve as the input of the attention module. After three-layer convolution, a one-channel attention map (a) is generated, which contains pixel-wise positions for object-related features. For feature selection, each channel of current feature map multiplies this attention map pixel-by-pixel, and the attention-aware feature ($a \circ x$) can be obtained. The attention-aware feature and previous hidden state are concatenated

as the input of the ConvLSTM. Different from traditional LSTM, gates (i, f, o) and incoming information (c) will be computed with convolution operation [13]. Subsequently, controlled by gates, the temporal memory (s) will be updated, and current hidden state is generated for multi-box regression and classification. During this operation, $a \circ x, i, f, o, c, s, h$ are in the same size. In addition, we also use dropout regularization [40] for the attention-aware feature during training. Apparently, temporal information transmission is conducted twice in temporal attention and ConvLSTM.

Note that the attention module and input gate play different roles, although both of them can be aware of useful features. For background suppression and scale suppression, the attention module works for spatial location in each 2-D map, whereas the input gate can deal with the 3-D feature along the channel to preserve discriminative data.

B. Training

We design a multi-task objective to train TSSD, including a localization loss \mathcal{L}_{loc} , a confidence loss \mathcal{L}_{conf} , an attention loss \mathcal{L}_{att} , and an association loss \mathcal{L}_{asso} ,

$$\mathcal{L} = \frac{1}{M}(\alpha\mathcal{L}_{loc} + \beta\mathcal{L}_{conf}) + \gamma\mathcal{L}_{att} + \xi\mathcal{L}_{asso}, \tag{2}$$

where M is the number of matched boxes, and $\alpha, \beta, \gamma, \xi$ are tradeoff parameters. In generally, \mathcal{L}_{loc} and \mathcal{L}_{conf} are defined in accordance with SSD [8].

Subsequently, we train TSSD through three steps.

1) *Attention Loss*: The generation of attention maps is supervised using cross entropy. At first, we construct the ground truth attention map A_g , in which elements in ground truth boxes equal to 1 and others are 0. There are six feature maps for multi-box prediction, which generate multi-scale attention maps A_{psc} . Therefore, each A_{psc} is firstly unified to the same resolution as the input image through bilinear upsampling operation, followed by the produce of A_{psc}^{up} . Then, \mathcal{L}_{att} can be given as,

$$\mathcal{L}_{att} = \sum_{sc=1}^6 \mu(-A_{psc}^{up} \log(A_g) - (1 - A_{psc}^{up}) \log(1 - A_g)), \tag{3}$$

where μ averages all elements in a matrix.

2) *Association Loss*: Pixel-level changes could significantly impact the detection results, so an object in video always encounters large score fluctuations with a static detection method (studied in [17]). Thus, towards temporal consistency of videos, an association loss should be developed for sequence training. To that end, we encourage the TSSD to generate similar global classification results for several consecutive frames. We firstly compute top k high predicted scores per class after NMS, then sum them to generate a class-discriminative score list (sl). The score list should remain small fluctuation in consecutive frames. Thereby, the \mathcal{L}_{asso} can be obtained by,

$$\mathcal{L}_{asso} = \left(\sum_{t=1}^{seq_len} sl_t - sl_{ave} \right) / seq_len, \tag{4}$$

where sl_t is the score list at time step t ; sl_{ave} denotes the mean score list among $sl_{1:t-1}$; and seq_len represents the sequence

length. It should be remarked that our proposed association loss belongs to a self-supervision method. That is, there is no incoming ground truth label when computing \mathcal{L}_{asso} .

3) *Multi-Step Training*: We first train an SSD model following [8]. In the next step, the TSSD is trained based on well-trained SSD. We freeze the weights in the network except for AC-LSTM and detection head (i.e., parameters for regression and classification). In particular, the ConvLSTM is trained with RMSProp [37] while the rest of TSSD is trained using SGD optimizer with the initial learning rate is 10^{-4} and a decay rate of 0.1 for 30 epochs. The total iteration number is 40 epochs at this training step. On the other hand, the TSSD should be trained with a sequence of frames, but the frame rates of videos are inconstant. Moreover, the motion speed of objects in videos is of a big difference. For better generalization, it should not be trained frame by frame. Instead, we only choose seq_len frames in a video for backpropagation in an iteration. The seq_len frames are chosen uniformly based on the start frame sf and skip sp , namely, random skip sampling (RSS), which can be formulated as,

$$\begin{aligned} sp &= R[1, v/seq_len] \\ sf &= R[1, v - seq_len \times sp + 1], \end{aligned} \quad (5)$$

where v is the total number of frames in a video, and $R[min, max]$ represents the operation of selecting an integer randomly between min and max . Finally, the uniform seq_len frames are chosen with sf as the start frame and sp as the skip. In this paper, $seq_len = 8$. At this step, the association loss \mathcal{L}_{asso} is not involved.

Thirdly, the full objective including \mathcal{L}_{asso} is used to fine tune parameters for 10 epoches. At this step, the learning rate is 10^{-5} , and $sp = 1$. The hyper parameters $\alpha = 1, \beta = 1, \gamma = 0.5, \xi = 2, \delta = 3$ are selected based on the performance of validation set.

C. Inference

At inference phase, the backbone and extra layers extract multi-scale features. Subsequently, the HL-TU and AC-LSTM integrate these features through time, generating temporally-aware hidden state for regression and classification. Finally, we apply the NMS with jaccard overlap (IoU) of 0.45 (for ImageNet VID) or 0.3 (for 2DMOT15) per class and retain the top 200 (for ImageNet VID) or 400 (for 2DMOT15) high confident detections per image to produce the final detection results.

D. Online Tubelets Analysis

For online tracking by detection task, it is expected that the TSSD is endowed with the ability of identifying. Tubelet in videos has been studied by [17], [21], [38], each of which has a unique ID. [17] generates tubelets by tracking, whereas [21] and [38] propose tubelets for batch-mode detection. However, these methods are either computationally expensive or not online. In another sphere, siamese network maps two targets on to a metric space, where the mapped features are always

Algorithm 1 Online Tubelet Analysis

```

1: for  $cls \in \text{classes}$  do
2:   if  $tubs[cls]$  is not empty then
3:     for  $obj \in \text{detection result}$  do
4:        $S_{obj}^{max} = 0$ 
5:       for  $tub \in tubes[cls]$  do
6:          $S_{obj,tub} = (7)$ 
7:         if  $S_{obj,tub} > S_{obj}^{max}$  then
8:            $S_{obj}^{max} = S_{obj,tub}$ 
9:            $candidate = tub$ 
10:        end if
11:      end for
12:      if  $S_{obj}^{max} > \mathcal{T}$  then
13:         $obj = obj^{candidate[id]}$ 
14:      end if
15:    end for
16:    for  $tub \in tubes[cls]$  do
17:      if  $\text{len}(obj^{tub[id]}) > 1$  then
18:        preserve only one with maximal  $S$ 
19:      end if
20:    end for
21:    for  $obj \in \{obj^{-1}\}$  do
22:      if  $obj[conf] > \mathcal{G}$  then
23:         $obj = obj^{new\_id}$ 
24:      end if
25:    end for
26:    update  $tubs[cls]$ 
27:  end if
28: end for

```

discriminative for each object [42]. Thereby, we attempt to introduce this framework to the TSSD.

Features in a detector are not suitable for identification, because they always contain within-class-similar information. Fortunately, there is a kind of category-independent feature in our framework, i.e., attention maps. Instead of being discriminative for each class, the our attention maps describe the object's prominence at different visual scales. Thereby, the attention space is creatively utilized for metric for fast data association. This idea is straightforward and computationally inexpensive, where the key intuition is that the prominence of objects are diverse from each other, and attention mechanism is able to catch this subtle distinctiveness. In reality, the low-level AC-LSTM is employed as a siamese network through time, because low-level features cover more detailed information. Then, the attention similarity $as_{i,j}$ between two objects i and j and the can be formulated as a cosine distance,

$$as_{i,j} = \frac{av_i \cdot av_j}{||av_i|| ||av_j||}, \quad (6)$$

where av denotes the 147-dimension attention vector unfolded by bilinear-sampled multi-scale attention maps.

Moreover, identification in a video can leverage more temporal coherence, so we also employ IoU o in the OTA. Due to multiple objects in a tubelet, the similarity $\mathcal{S}_{i,tub}$ between

an object obj and a tubelet tub can be given as,

$$\begin{aligned} as_{obj,tub} &= (\sum_{k \in tub} as_{obj,k}) / tub_len \\ o_{obj,tub} &= \text{IoU}(obj, tub[0]) \\ \mathcal{S}_{obj,tub} &= \exp(o_{obj,tub}) \times as_{obj,tub}, \end{aligned} \quad (7)$$

where tub_len is current length of the tubelet, and $tub[0]$ denotes the most recent object.

Define \mathcal{G}, \mathcal{T} to denote the tubelet generation score, match threshold, respectively. Suppose that each detected object is described as $obj[conf, loc, av]$, and each class-distinct tubelets set is denoted as $tubs[cls]$, each tubelet in which is given as $tub[id, objs]$, the OTA algorithm is presented in Algorithm 1, where obj^{id} denotes an object with an identify id , and $id = -1$ represents an object without an identify. $len(\cdot)$ computes the number of elements. Note that the maximal existence time after disappearance and maximal tubelet length are restricted when tubelets are updated.

IV. EXPERIMENT AND DISCUSSION

A. Dataset

1) *ImageNet VID*: We evaluate TSSD on the ImageNet VID dataset [26], which is the biggest dataset for temporal object detection now. The task requires algorithms detect 30-class targets in consecutive frames. There are 4000 videos in the training set, containing 1181113 frames. On the other hand, the validation set compasses 555 videos, including 176126 frames. We measure performance as mean average precision (mAP) over the 30 classes on the validation set following [3], [8]. In addition, ImageNet DET dataset is employed as training assistance. The 30 categories in VID dataset are a subset of the 200 categories in the DET dataset. Therefore, following [16], [17], [21], [22], we train the SSD with VID and DET (only using the data from the 30 VID classes). In reality, there are millions of frames in VID training set, so it is hard to train a network directly using them. Additionally, the data for each category are imbalanced, because there are long videos (contain more than 1000 frames) and short videos (contain only a dozen frames). Thus, following [22], we sample at most 2000 images per class from DET, and select 10 frames in each VID video for SSD training at the first step. In the second and third training steps, all the VID training videos are adopted.

2) *2DMOT15*: The TSSD-OTA is an identity-aware detector, so 2DMOT15 dataset [43] is employed to evaluate tracking performance. This is a multi-object tracking consisting of 11 training sequences. Since the annotations are available for the training set only, we split 5 videos as the validation set following [24]. In addition, another 3 video sequences in MOT17Det [44] dataset are employed for training.

B. Runtime Performance

Our methods are implemented under the PyTorch framework. The training and experiments are carried out on a workstation with an Intel 2.20 GHz Xeon(R) E5-2630 CPU, NVIDIA TITAN-X GPUs, 64 GB of RAM, CUDA 8.0, and cuDNN v6. The inference time is described in Table I, and

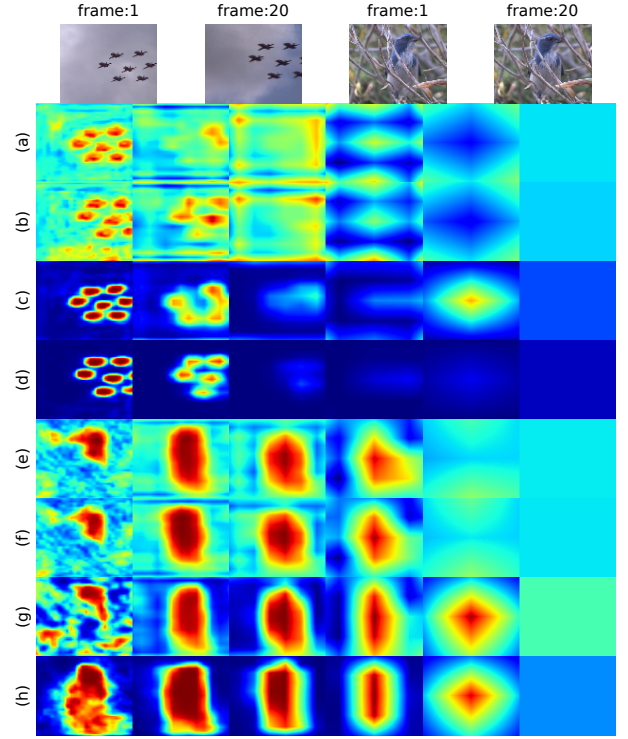


Fig. 4. Effect of the ConvLSTM for attention module. There are two video snippets containing small objects (airplane) or wild environment (bird). The traditional attention and temporal attention module are used to generate multi-scale attention maps, in which crimson denotes higher level of concern while mazarine represents something neglected. (a)–(b) attention maps for airplanes generated by traditional module; (c)–(d) attention maps for airplanes generated by temporal module; (e)–(f) attention maps for bird generated by traditional module; (g)–(h) attention maps for bird generated by temporal attention module; In above 4 pairs maps, the former is for the first frame while the latter is with respect to the 20th frames. Each line in (a)–(h) is multi-scale attention maps. From left to right, they are responsible for *Conv4_3*, *Conv7*, *Conv8_2*, *Conv9_2*, *Conv10_2*, *Conv11_2*, respectively. This figure is best viewed in color.

we achieve a beyond real-time speed for temporal detection or tracking.

TABLE I
FPS LIST ON EMPLOYED DATASETS BY THE PROPOSED METHODS.

Method	VID (FPS)	2DMOT15 (FPS)
SSD	~ 45	~ 77
TSSD	~ 27	~ 30
TSSD-OTA	~ 21	~ 27

C. Ablation Study on ImageNet VID

Our methods progressively improve the object detection performance.

1) *HL-TU*: Our proposed HL-TU is effective in the following aspects. Firstly, redundant parameters are avoided. For example, the original SSD contains 2.6 M parameters, and SSD with HL-TU has 4.9 M parameters. However, if six ConvLSTMs are employed for each feature map, the amount of parameter will dramatically increase to 15.5M. Secondly, as reported in [24], *Conv4_3* and *Conv11_2* make relatively

TABLE II
EFFECTIVENESS OF VARIOUS DESIGNS. ALL MODEL ARE TRAINED AND VALIDATED ON IMAGENET VID DATASET.

Component	TSSD					
Association loss?	✓					
The 3rd training stage?	✓	✓				
RSS in the 2nd stage?	✓	✓	✓			
AC-LSTM?	✓	✓	✓	✓		
HL-TU?	✓	✓	✓	✓	✓	
mAP(%)	65.43	65.13	64.76	64.63	63.95	63.03

TABLE III
COMPARISON OF THE TSSD AND SEVERAL PRIOR AND CONTEMPORARY APPROACHES.

Method	Components								Performances			
	1-stage	2-stage	Backbone	Optical flow	Track	Attention	RNN		Real time	Online	ID	mAP
TCNN [17]		✓	DeepID+Craft [31], [32]	✓	✓					✓		61.5
TPN [21]		✓	GoogLeNet [33]				✓					68.4
D&T [22]		✓	ResNet-101 [34]		✓					✓		79.8
FGFA [29]		✓	ResNet-101	✓						✓		76.3
STSN [39]		✓	ResNet-101									78.7
HPVD [41]		✓	ResNet-101	✓								78.6
Object-link [38]		✓	ResNet-101							✓		80.6
Closed-loop [19]		✓	VGG-M [30]							✓		50.0
STMN [27]		✓	VGG-16				✓					55.6
Seq-NMS [18]			VGG-16							✓		52.2
LSTM-SSD [28]	✓		MobileNet [35]				✓	✓	✓	✓		54.4
TSSD(-OTA)	✓		VGG-16			✓	✓	✓	✓	✓	✓	65.4

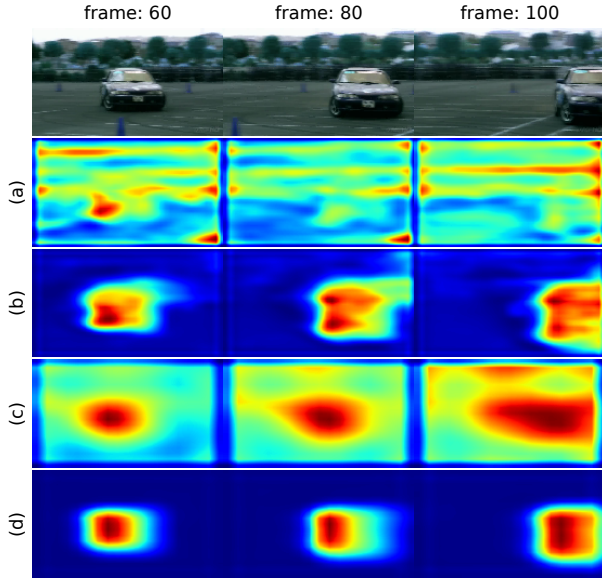


Fig. 5. Effect of the temporal attention for ConvLSTM. The ConvLSTM's memory (s) is visualized (by computing the L2 norm across feature channels at each spatial location to get a saliency map). (a) original ConvLSTM's memory for *Conv4_3*; (b) ConvLSTM's memory for *Conv4_3* in AC-LSTM; (c) original ConvLSTM's memory for *Conv7*; (d) ConvLSTM's memory for *Conv7* in AC-LSTM. This figure is best viewed in color.

less contribution to detection. That is, there are a small amount of data for oversized or tiny-size objects. Thus, the highest-level and lowest-level ConvLSTMs can hardly be well trained, if six-scale ConvLSTMs are employed. We find that the

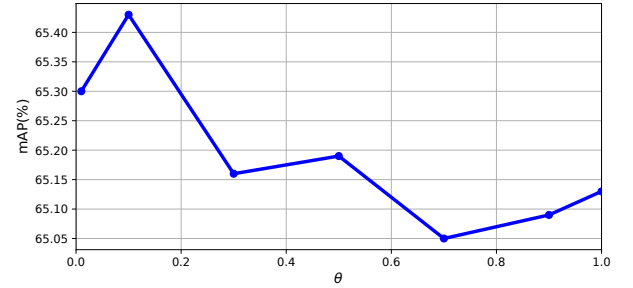


Fig. 6. Detection performance vs. θ . This figure shows model performance as a function of the confidence threshold θ in association loss.

mAP increases by 0.92% when HL-TU is adopted using two ConvLSTMs as temporal units due to the feature integration brought by ConvLSTMs.

2) *AC-LSTM*: At first, we qualitatively analyze the interaction of attention module and ConvLSTM. As shown in Fig. 4, the comparison of temporal and traditional attention modules are presented. Note that the traditional attention module only uses current feature map as the input. As for presented heat maps in Fig. 4, crimson means a higher probability of being a target, whereas the mazarine indicates ignorable pixel position in feature maps. Moreover, multi-scale attention maps are generated in the TSSD, and the righter maps response higher-level features. For the ease of observation, the multi-scale attention maps have been unified to the same spatial resolution as the input image through a bilinear upsampling operation.

We choose two challenging scenes in this test. The airplane frames include small objects, and the bird frames contain rich

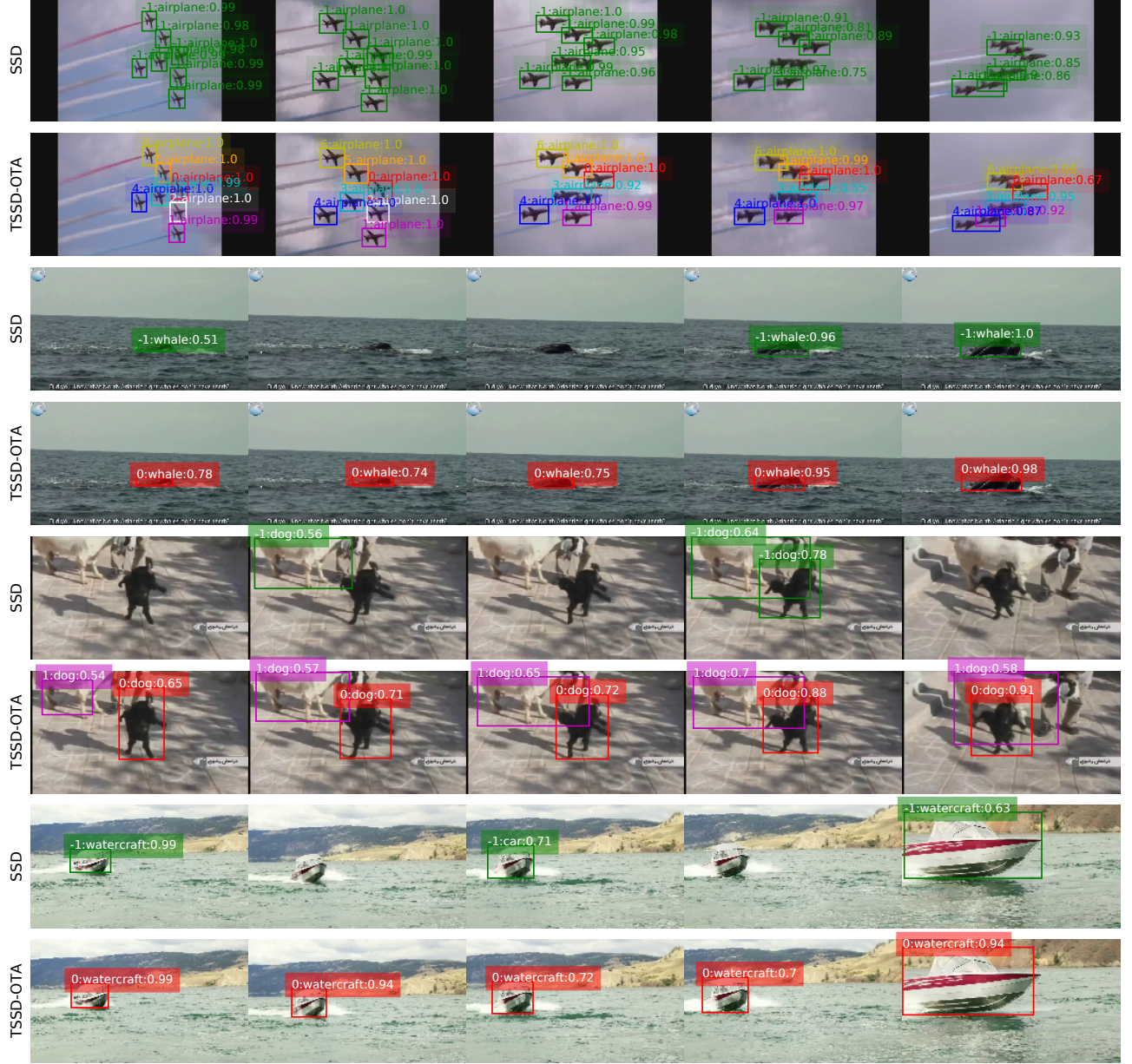


Fig. 7. Demonstration results on the ImageNet VID validation dataset. The proposed TSSD(-OTA) can handle a variety of scenes with multiple objects more accurately. In addition, different from traditional detector, our approach has capability of identifying. The detection results are shown as “ID : Class : Score”. ID = -1 means the identity is not generated. This figure is best viewed in color.

stripes, both of which are difficult for attention operation. As shown in Fig. 4(a), (b), (e), (f), the original attention method is not able to handle these two scenes. That is, although the targets are focused roughly, the background and small-contributed multi-scale feature maps are not suppressed effectively. Moreover, there is no improvement through time series. On the contrary, as illustrated in Fig. 4(c), (d), (g), (h), the proposed attention module performs better. In short, our method not only localizes the targets more accurately, but also suppresses the background more efficiently. Further, our method is effective for scale suppression. For instance, small objects in airplane frames are detected by *Conv4_3*. As shown in Fig. 4(d), the attention maps for *Conv4_3*, *Conv7* localize

airplanes, and all the last four maps are “cold”. That is, when it comes to larger scale, our attention module can not find any target, so the whole of feature map has been suppressed. In addition, the performance of proposed approach improves along with the accumulation of temporal information. For example, in Fig. 4(g), (h), the attention map for *Conv4_3* can hardly find the bird in the first frame, but the bird’s profile is focused without overmuch background in the 20th frame. Moreover, if attention maps for the first frame are compared, a conclusion can be drawn that the temporal attention module is better even though the temporal information has not generated. The reason is that temporal attention model can be trained more effectively.

On the other hand, there are benefits of the AC-LSTM over traditional ConvLSTM. Referring to Fig. 5, the ConvLSTM’s memories for *Conv4_3*, *Conv7* are visualized. Small-scale memory deals with image details, but ConvLSTM can not generate valid memory because it is confused by mussy features, whereas AC-LSTM is able to memorize the essential information of the car without background (see Fig. 5(a–b)). In consideration of the scale of the car, *Conv7* is more crucial to detecting it. As shown in Fig. 5(c), the ConvLSTM for *Conv7* has the tendency to learn trivial representations that just memorize the inputs. Moreover, this memorization also involves the background. Thus, not all these information is useful for future detection, and they may incur inaccuracies. On the contrary, the AC-LSTM produces more clear memory with pivotal features (see Fig. 5(d)).

Due to the above reasons, the improvement brought by AC-LSTM is evident, i.e., the mAP rises by 1.74% based on that of SSD.

3) *Association Loss*: The association loss is adopted in the third training stage, where $sp = 1$ assuring the training data is highly associated. Without the association loss, we obtain 65.13% as an mAP after fine tune, but \mathcal{L}_{asso} can make further improvement. In consideration of the employed NMS, there are three parameter settings for computing association loss, i.e., confidence threshold θ , IoU threshold, and top k retained boxes. Because of the NMS, the number of retained boxes is relatively insensitive, and the IoU threshold could be consistent with that in the inference phase. Thus, the major implication of \mathcal{L}_{asso} is θ , which indicates what kind of objects need to be involved. In this experiment, we set $k = 75$ to explore the impact of θ . As depicted in Fig. 6, the mAP generally decreases as θ increasing. Overmuch invalid boxes are considered when $\theta = 0.01$, whereas the \mathcal{L}_{asso} gradually loses efficacy as θ increasing. Hence, taking into account almost all positive samples, \mathcal{L}_{asso} is the most effective when $\theta = 0.1$. Consequently, the TSSD achieves 65.43% as an mAP.

4) *Comparison with Other Architectures*: We also compare the TSSD against several prior and contemporary approaches. As shown in Table III, their components and performances have been summarized. Most methods are based on a two-stage detector with RPN for region proposal, and few approaches successfully adopt attention or LSTM for temporal coherence. On the other hand, tracking employed in TCNN [17] and D&T [22] is a good idea for video detection, but it affects time efficiency to some extent. Some approaches process video sequences in a batch mode, where further frames are also utilized for current frame detection. Hence, such non-causal methods are prohibitive for real-world application. Because of its real-time and online characteristic, the TSSD is able to detect objects temporally for real world applications. According to the authors’ knowledge, our method has the following merits:

- The TSSD is the first temporal one-stage detector achieving above 65% mAP with such small input image and VGGNet as a backbone.
- The TSSD-OTA is a unified framework, where a real-time online detector is capable of identifying objects.

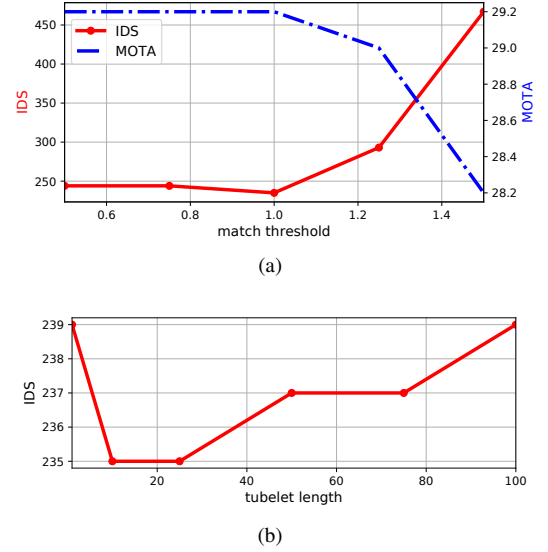


Fig. 8. Tracking performance v.s. \mathcal{T} , tub_len .

TABLE IV
EFFECTIVENESS OF ATTENTION MAPS FOR IDS. THE CHECKMARK INDICATES THAT CORRESPONDING ATTENTION MAP IS EMPLOYED TO COMPUTE S .

<i>Conv4_3</i>	<i>Conv7</i>	<i>Conv8_2</i>	<i>Conv9_2</i>	<i>Conv10_2</i>	IDS
					550
✓					236
	✓				240
		✓			238
			✓		244
				✓	251
✓	✓				236
✓	✓	✓			235
✓	✓	✓	✓		236
✓	✓	✓	✓	✓	237

This framework is absent in the existing video detection approaches.

5) *Qualitative Results*: We show some qualitative results on the ImageNet VID validation set in Fig. 7. We only display the detected bounding boxes with the score larger than 0.5. Different colors of the bounding boxes indicate different object identity. The proposed TSSD works well with precision and temporal stability.

D. Tracking Performance on 2DMOT15 Dataset

We employ the 2DMOT15 dataset to jointly investigate the TSSD and OTA, whose metrics are designed for tracking. MOTA considers the comprehensive detection and tracking performance, and MOTP measures the tightness of the tracking results and ground truth. FP, PN denote the total number of false positives and false negatives, respectively. For each trajectory, if more than 80% of positions are successfully tracked, MT increases by 1. On the other hand, if less than 80% of positions are lost, ML increases by 1. Finally, IDS counts ID switch times.

1) *Parameter Analysis*: There are three parameters in OTA, i.e., match threshold \mathcal{T} , tubelet generation score \mathcal{G} , and tubelet length tub_len . To track each detected object, \mathcal{G} should equal

TABLE V
TRACKING PERFORMANCE ON THE 2DMOT15 VALIDATION SET.

Method	MOTA \uparrow	MOTP \uparrow	MT \uparrow	ML \downarrow	FP \downarrow	FN \downarrow	IDS \downarrow	FPS \uparrow
ACF-MDP [45], [48]	26.7	73.6	12.0%	51.7%	3290	13491	133	$\sim < 1/1$
SSD-ALSTM [24]	38.6	74.2	14.9%	46.8%	788	13253	154	$\sim 9/12$
FasterRCNN-SORT [47]	34.0	73.3	20.5%	32.1%	3311	11660	274	$\sim 5/220$
TSSD-SORT	25.6	72.4	6.4%	48.9%	798	16121	260	$\sim \mathbf{28/420}$
TSSD-OTA(proposed)	29.2	71.9	12.4%	34.6%	1482	14624	235	$\sim 27/270$

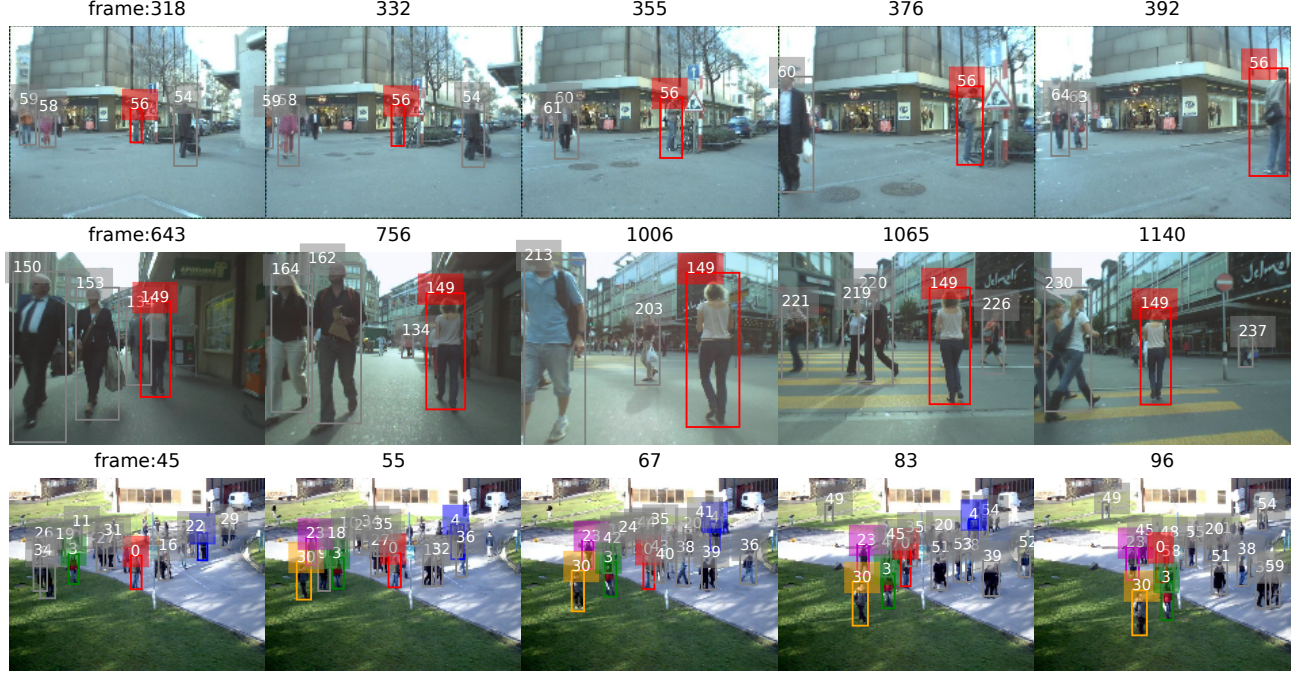


Fig. 9. Demonstration results on the 2DMOT15 validation dataset. The proposed TSSD-OTA can track pedestrians in a variety of multi-target scenes. The identities for each object are denoted on boxes, and some representative results are demonstrated in red, green, blue, or orange. This figure is best viewed in color.

to detector's confidence threshold $conf$, and \mathcal{T}, tub_len will impact the tracking performance. We let $conf = \mathcal{G} = 0.3, tub_len = 10$ to investigate the effect of \mathcal{T} . The change of MOTA and IDS is employed to represent the impact of tracking performance here. Referring Fig. 8(a), MOTA and IDS are strongly influenced by \mathcal{T} , and $\mathcal{T} = 1.0$ is optimal as for our validation set. That is, if \mathcal{T} is too high, the number of the failed match will increase. On the other hand, lower \mathcal{T} causes the false match. Both failed and false match can weaken tracking performance. However, as shown in Fig. 8(a), failed match has a greater implication, because S_{obj}^{max} prevents OTA from overmuch false match. as illustrated in Fig. 8(b), IDS also first decreases and then increases as tub_len rising ($\mathcal{T} = 1.0$). If $tub_len = 1$, the match process only relies on the most recent object, so it is unreliable for some emergencies (e.g., occlusion). However, an oversized tub_len would retain remote information, which may result in inaccurate.

We also unveil the effectiveness of attention maps for IDS with the parameters of $conf = \mathcal{G} = 0.3, tub_len = 10, \mathcal{T} = 1.0$. Note that the attention map for *Conv11_2*, whose size is 1×1 , is not qualified for identification, so it is not been

involved in this test. Referring Table IV, IDS is equal to 550 when \mathcal{S} is computed with IoU alone ($\mathcal{T} = 0.5, \mathcal{S} = o$ here). The validity of attention maps is evident, and IDS drops about 60% as a result. In addition, the effectiveness gradually declines as visual scale increasing, since high-level features usually contain more within-class-similar information. Further, we also combine multi-scale attention maps to compute \mathcal{S} , and the best result is obtained when attention maps in low-level AC-LSTM are employed.

2) *Tracking Results*: Under the conditions of $tub_len = 10, \mathcal{T} = 1.0, conf = \mathcal{G} = 0.3$, we use the TSSD-OTA to track pedestrian in 2DMOT15 dataset.

Referring to Table V, the FPS is described in the form of *overall speed / tracking component speed*. A conclusion can be drawn based on the comparison with prior and contemporary approaches that the proposed TSSD-OTA can run at frame-rates beyond real time while maintaining comparable tracking performance. Concerning MT and ML, the FasterRCNN-SORT performs better because the two-stage detector works well on recall rate. In case of MOTA, the SSD-ALSTM is better owing to the LSTM in tracking components. However,

their solutions comes with a major drawback, i.e., high time cost. There are two main reasons causing the proposed TSSD-OTA can not be equal to the compared methods on some criteria. i) There are vast small objects in the 2DMOT15 dataset, but our detector with such small input image is not adept at dealing them; ii) Unlike tracking method, our model is optimized without any objective related to identity or association. The proposed association loss is also not adopted in this experiment, and we will explain the reason in Section IV-E.

Then, employing TSSD as the detector, we compare OTA and SORT [47] comprehensively. As shown in Table V, we achieve better indexes on MOTA, MT, ML, FN, and IDS. That is, the OTA generates better tracking performance while keeping quite high processing speed.

3) *Qualitative Results*: As schematically illustrated in Fig. 9, the proposed TSSD-OTA is able to track pedestrians in a variety of scenarios. We select some typical results for demonstration. In the first line of Fig. 9, #56 is in a small size at the beginning, then it becomes larger with the change of visual perspective. As a result, the TSSD-OTA can adapt to this continuous scale change. #149 in the second line shuttles in the crowd. Moreover, it undergoes illumination changes. Still, this challenging target is tracked well by the TSSD-OTA. There are chaotic small objects in the third line of Fig. 9, and they occlude each other. However, our method works well in terms of #0, #3, #4, #23, #30, and etc.. Unfortunately, there are some failed cases appear in this complex scenario, e.g., ID switches (#15→#39, #26→#23, #34→#30), false negatives (#4, #49).

E. Discussion

Although above experiment and analysis cover almost all aspects of our proposed approaches, we also discuss two crucial yet usually ignored components in combination with two datasets, i.e., RSS and association loss. We employ ImageNet VID and 2DMOT15 datasets for experiments, which are significantly different as for data amount (4000 v.s. 8), class number (30 v.s. 1), and metrics (mAP v.s. MOTA and etc.). In addition, 2DMOT15 contains vast small objects while VID covers multifarious scenarios. Still, our proposed TSSD-OTA can handle them well concerning detection accuracy, inference speed, and tracking performance.

As shown in Table II, there are only 0.14% mAP increase after RSS is adopted. However, the reduced data amount highlights the need for it. For example, the TSSD can not be well trained without RSS on the 2DMOT15 dataset, and the MOTA dramatically decrease to -135.5 as a consequence. Obviously, the phenomenon is caused by the diversity of training data. That is, due to a variety of scenarios in VID dataset, the data diversity can be preserved without RSS. Unfortunately, this trick can not be neglected when training 2DMOT15 dataset, since there are only 8 employed videos. Since our association loss requires continuous sampling, it is not adopted during 2DMOT15 training.

It is not the first time that an association loss is designed. For instance, Lu et al. also exploited one to train a LSTM [24].

As opposed to previous design, our association loss focuses global classification rather than each associated object pair. By this mean, we do not introduce identity ground truth label to the training process. It is necessary because detection datasets usually do not involve the identity label, or collecting ID-labelled data is a costly work.

V. CONCLUSION AND FUTURE WORK

This paper has aimed at temporally detecting and identifying objects in real time for real-world applications. A creative TSSD is proposed. Differing from existing video detection methods, the TSSD is a temporal one-stage detector, and it can perform well in terms of both detection precision and inference speed. To efficiently integrate pyramidal feature hierarchy, an HL-TU is proposed, in which the high-level features and low-level features share their respective temporal units. Furthermore, we design an AC-LSTM as a temporal analysis unit, where the temporal attention module is responsible for background suppression and scale suppression. A novel association loss function and multi-step training are also designed for sequence learning. In addition, the OTA algorithm equips TSSD with the ability of identification with low computational costs. As a result, the TSSD-OTA sees considerably enhanced detection precision, tracking performance, and inference speed.

In the future, we plan to investigate the stability of temporal detection and tracking. Besides, the TSSD-OTA will be used for robotic visual navigation under dynamic environments.

REFERENCES

- [1] R. Girshick, J. Donahue, T. Darrell, and J. Malik, "Rich feature hierarchies for accurate object detection and semantic segmentation," in *Proc. IEEE Conf. Comput. Vis. Pattern Recognition*, Columbus, U.S., Jun. 2014, pp. 580–587.
- [2] R. Girshick, "Fast R-CNN," in *Proc. IEEE Int. Conf. Comput. Vis.*, Santiago, Chile, Dec. 2015, pp. 1440–1448.
- [3] S. Ren, K. He, R. Girshick, and J. Sun, "Faster R-CNN: Towards real-time object detection with region proposal networks," in *Proc. Adv. in Neural Info. Proc. Syst.*, Montreal, Canada, Dec. 2015, pp. 91–99.
- [4] K. He, G. Gkioxari, P. Dollár, and R. Girshick, "Mask R-CNN," Venice, Italy, Oct. 2017, pp. 2961–2969.
- [5] J. Dai, Y. Li, K. He, and J. Sun, "R-FCN: Object detection via region-based fully convolutional networks," in *Proc. Adv. in Neural Info. Proc. Syst.*, Barcelona, Spain, Dec. 2016, pp. 379–387.
- [6] T. Y. Lin, P. Dollár, R. Girshick, K. He, B. Hariharan, and S. Belongie, "Feature pyramid networks for object detection," in *arXiv:1612.03144*, 2016.
- [7] J. Redmon, S. Divvala, R. Girshick, and A. Farhadi, "You only look once: Unified, real-time object detection," in *Proc. IEEE Conf. Comput. Vis. Pattern Recognition*, Las Vegas, U.S., Jun. 2016, pp. 779–788.
- [8] W. Liu, D. Anguelov, D. Erhan, C. Szegedy, S. Reed, C. Y. Fu, and A. C. Berg, "SSD: Single shot multibox detector," in *Proc. Eur. Conf. Comput. Vis.*, Amsterdam, Netherlands, Oct. 2016, pp. 21–37.
- [9] T. Y. Lin, P. Goyal, R. Girshick, K. He, and P. Dollár, "Focal loss for dense object detection," Venice, Italy, Oct. 2017, pp. 2980–2988.
- [10] Y. Zhang, M. Pezeshki, P. Brakel, S. Zhang, C. L. Y. Bengio, and A. Courville, "Towards end-to-end speech recognition with deep convolutional neural networks," *arXiv:1701.02720*, 2017.
- [11] I. Sutskever, O. Vinyals, and Q. V. Le, "Sequence to sequence learning with neural networks," in *Proc. Adv. in Neural Info. Proc. Syst.*, Montreal, Canada, Dec. 2014, pp. 3104–3112.
- [12] S. Hochreiter and J. Schmidhuber, "Long short-term memory," *Neural Comput.*, vol. 9, no. 8, pp. 1735–1780, 1997.
- [13] X. Shi, Z. Chen, H. Wang, D. Yeung, W. Wong, and W. Woo, "Convolutional LSTM network: A machine learning approach for precipitation nowcasting," in *Proc. Adv. in Neural Info. Proc. Syst.*, Montreal, Canada, Dec. 2015, pp. 802–810.

- [14] S. Valipour, M. Siam, M. Jagersand, and N. Ray, "Recurrent fully convolutional networks for video segmentation," *arXiv:1606.00487*, 2016.
- [15] V. Mnih, N. Heess, and A. Graves, "Recurrent models of visual attention," in *Proc. Adv. in Neural Info. Proc. Syst.*, Montreal, Canada, Dec. 2014, pp. 2204–2212.
- [16] K. Kang, W. Ouyang, H. Li, and X. Wang, "Object detection from video tubelets with convolutional neural networks," in *Proc. IEEE Conf. Comput. Vis. Pattern Recognition*, Las Vegas, U.S., Jun. 2016, pp. 817–825.
- [17] K. Kang, H. Li, J. Yan, X. Zeng, B. Yang, T. Xiao, C. Zhang, Z. Wang, R. Wang, X. Wang, and W. Ouyang, "T-CNN: Tubelets with convolutional neural networks for object detection from videos," *IEEE Trans. Circuits Syst. Video Technol.*, DOI:10.1109/TCSVT.2017.2736553.
- [18] W. Han, P. Khorrami, T. L. Paine, P. Ramachandran, M. Babaeizadeh, H. Shi, J. Li, S. Yan, and T. S. Huang, "Seq-NMS for video object detection," *arXiv:1602.08465*, 2016.
- [19] L. Galteri, L. Seidenari, M. Bertini, and A. Del Bimbo, "Spatio-temporal closed-loop object detection," *IEEE Trans. Image Process.*, vol. 26, no. 3, pp. 1253–1263, 2017.
- [20] S. Tripathi, S. Belongie, Y. Hwang, and T. Nguyen, "Detecting temporally consistent objects in videos through object class label propagation," in *Proc. IEEE Winter Conf. Appl. Comput. Vis.*, New York, U.S., Mar. 2016, pp. 1–9.
- [21] K. Kang, H. Li, T. Xiao, W. Ouyang, J. Yan, X. Liu, and X. Wang, "Object detection in videos with tubelet proposal networks," in *Proc. IEEE Conf. Comput. Vis. Pattern Recognition*, Hawaii, U.S., Jul. 2017, pp. 727–735.
- [22] C. Feichtenhofer, A. Pinz, and A. Zisserman, "Detect to track and track to detect," in *Proc. IEEE Conf. Comput. Vis. and Pattern Recognition*, Venice, Italy, Oct. 2017, pp. 3038–3046.
- [23] G. Ning, Z. Zhang, C. Huang, X. Ren, H. Wang, C. Cai, and Z. He, "Spatially supervised recurrent convolutional neural networks for visual object tracking," in *Proc. IEEE Int. Symp. Circuits and Syst.*, Baltimore, the US, May. 2017, pp. 1–4.
- [24] Y. Lu, C. Lu, and C. K. Tang, "Online video object detection using association LSTM, in *Proc. IEEE Int. Conf. Comput. Vis.*, Venice, Italy, Oct. 2017, pp. 2344–2352.
- [25] K. Simonyan and A. Zisserman, "Very deep convolutional networks for large-scale image recognition," *arXiv:1409.1556*, 2014.
- [26] O. Russakovsky, J. Deng, H. Su, J. Krause, S. Satheesh, S. Ma, Z. Huang, A. Karpathy, A. Khosla, M. Bernstein, A. C. Berg, and F. Li, "ImageNet large scale visual recognition challenge," *Int. J. Comput. Vis.*, vol. 115, no. 3, pp. 211–252, 2015.
- [27] F. Xiao and Y. J. Lee, "Spatial-temporal memory networks for video object detection," *arXiv:1712.06317*, 2017.
- [28] M. Liu and M. Zhu, "Mobile video object detection with temporally-aware feature maps," *arXiv:1711.06368*, 2017.
- [29] X. Zhu, Y. Wang, J. Dai, L. Yuan, and Y. Wei, "Flow-guided feature aggregation for video object detection," *arXiv:1703.10025*, 2017.
- [30] K. Chatfield, K. Simonyan, A. Vedaldi, and A. Zisserman, "Return of the devil in the details: Delving deep into convolutional nets," in *Proc. Brit. Mach. Vis. Conf.*, Nottingham, the U.K., Sept. 2014, pp. 1–12.
- [31] W. Ouyang, P. Luo, X. Zeng, S. Qiu, Y. Tian, H. Li, S. Yang, Z. Wang, Y. Xiong, and C. Qian et al., "Deepid-net: multi-stage and deformable deep convolutional neural networks for object detection," *arXiv:1409.3505*, 2014.
- [32] B. Yang, J. Yan, Z. Lei, and S. Z. Li, "Craft objects from images," in *Proc. IEEE Conf. Comput. Vis. and Pattern Recognition*, Las Vegas, U.S., Jun. 2016, pp. 6043–6051.
- [33] C. Szegedy, W. Liu, Y. Jia, P. Sermanet, S. Reed, D. Anguelov, D. Erhan, V. Vanhoucke, and A. Rabinovich, "Going deeper with convolutions," in *Proc. IEEE Conf. Comput. Vis. and Pattern Recognition*, Boston, U.S., Jun. 2015, pp. 1–9.
- [34] K. He, X. Zhang, S. Ren, and J. Sun, "Deep residual learning for image recognition," in *Proc. IEEE Conf. Comput. Vis. and Pattern Recognition*, Las Vegas, U.S., Jun. 2016, pp. 770–778.
- [35] A. Howard, M. Zhu, B. Chen, D. Kalenichenko, W. Wang, T. Weyand, M. Andreetto, and H. Adam, "Mobilenets: efficient convolutional neural networks for mobile vision applications," *arXiv:1704.04861*, 2017.
- [36] D. S. Bolme, J. R. Beveridge, B. A. Draper, and Y. M. Lui, "Visual object tracking using adaptive correlation filters," in *Proc. IEEE Conf. Comput. Vis. Pattern Recognition*, San Francisco, U.S., Jun. 2010, pp. 2544–2550.
- [37] T. Tieleman and G. Hinton, "Lecture 6.5-rmsprop: Divide the gradient by a running average of its recent magnitude," *COURSERA: Neural Networks for Machine Learning*, vol. 4, no. 2, pp. 26–31, 2012.
- [38] P. Tang, C. Wang, X. Wang, W. Liu, W. Zeng, and J. Wang, "Object detection in videos by short and long range object linking," *arXiv:1801.09823*, 2018.
- [39] G. Bertasius, L. Torresani, and J. Shi, "Object detection in video with spatiotemporal sampling networks," *arXiv:1803.05549*, 2018.
- [40] N. Srivastava, G. E. Hinton, A. Krizhevsky, I. Sutskever, and R. Salakhutdinov, "Dropout : a simple way to prevent neural networks from overfitting," *J. Mach. Learn. Res.*, vol. 15, no. 1, pp. 1929–1958, 2014.
- [41] X. Zhu, J. Dai, L. Yuan, and Y. Wei, "Towards High Performance Video Object Detection," *arXiv:1711.11577*, 2017.
- [42] S. Chopra, R. Hadsell, and Y. LeCun, "Learning a similarity metric discriminatively, with application to face verification," in *Proc. IEEE Conf. Comput. Vis. Pattern Recognition*, San Diego, U.S., Jun. 2005, pp. 539–546.
- [43] L. Leal-Taixe, A. Milan, I. Reid, S. Roth, and K. Schindler, "MOTchallenge 2015: Towards a benchmark for multi-target tracking," *arXiv:1504.01942*, 2015.
- [44] A. Milan, L. Leal-Taixe, I. Reid, S. Roth, and K. Schindler, "MOT16: A Benchmark for Multi-Object Tracking," *arXiv:1603.00831*, 2016.
- [45] Y. Xiang, A. Alahi, and S. Savarese, "Learning to track: Online multi-object tracking by decision making," in *Proc. IEEE Int. Conf. Comput. Vis.*, Santiago, Chile, Dec. 2015, pp. 4705–4713.
- [46] H. U. Kim and C. S. Kim, "CDT: Cooperative detection and tracking for tracing multiple objects in video sequences. in *Proc. Eur. Conf. Comput. Vis.*, Amsterdam, Netherlands, Oct. 2016, pp. 851–867.
- [47] A. Bewley, Z. Ge, L. Ott, F. Ramos, and B. Upcroft, "Simple online and realtime tracking," in *IEEE Int. Conf. Image Process.*, Phoeix, U.S., Sept. 2016, pp. 3464–3468.
- [48] P. Dollar, R. Appel, S. Belongie, and P. Perona, "Fast feature pyramids for object detection," *IEEE Trans. Pattern Anal. Mach.*, vol. 36, no. 8, pp. 1532C1545, 2014.
- [49] R. Kalman, "A New Approach to Linear Filtering and Prediction Problems," *Journal of Basic Engineering*, vol. 82, no. Series D, pp. 35C45, 1960.
- [50] H. W. Kuhn, "The Hungarian method for the assignment problem," *Naval Research Logistics Quarterly*, vol. 2, pp. 83C97, 1955.

TABLE VI
AP LIST ON IMAGENET VID VALIDATION SET BY THE PROPOSED METHOD AND COMPARED METHODS.

Method	airplane	antelope	bear	bicycle	bird	bus	car	cattle	dog	d.cat	elephant
SSD	82.01	72.67	71.62	60.19	65.54	68.77	56.86	59.79	47.69	63.88	72.48
ConvLSTM	79.86	75.06	68.75	62.60	63.38	69.08	59.78	58.34	48.96	63.66	69.97
AC-LSTM	82.16	76.03	68.88	61.57	66.26	70.04	59.39	67.07	49.18	63.29	71.55
TSSD	81.53	76.55	68.32	64.04	66.29	68.89	60.18	65.11	49.83	64.88	71.72
Method	fox	g.panda	hamster	horse	lion	lizard	monkey	m.bike	rabbit	r.panda	sheep
SSD	77.47	79.04	89.04	61.53	26.43	61.34	41.78	73.58	49.20	20.96	58.99
ConvLSTM	80.61	78.03	90.12	62.53	28.17	62.15	41.25	75.69	54.33	44.90	56.19
AC-LSTM	80.85	80.71	90.18	63.36	30.21	64.61	41.50	75.81	56.00	39.85	57.26
TSSD	82.27	80.28	90.23	63.48	31.76	62.97	43.23	77.81	55.78	45.34	58.84
Method	snake	squirrel	tiger	train	turtle	w.craft	whale	zebra	FPS	mAP(%)	
SSD	47.95	47.11	80.71	76.98	69.07	61.61	63.54	83.34	~45	63.04	
ConvLSTM	46.41	45.95	81.18	76.03	70.33	62.56	58.65	83.96	~38	63.95	
AC-LSTM	49.34	46.41	82.45	77.68	71.49	62.02	54.58	83.20	~27	64.76	
TSSD	48.72	49.34	82.29	77.49	72.47	61.26	58.28	83.84	~27	65.43	

TABLE VII
TRACKING PERFORMANCE IN TERMS OF EACH VALIDATION VIDEO.

Video	MOTA \uparrow	MOTP \uparrow	MT \uparrow	ML \downarrow	FP \downarrow	FN \downarrow	IDS \downarrow
TUD-Campus	62.1	75.2	62.5%	0.0%	20	105	11
ETH-Sunnyday	52.8	72.3	13.3%	16.7%	149	705	23
ETH-Pedcross2	40.3	73.5	10.0%	36.8%	224	3430	88
ADL-Rundle-8	15.0	68.4	21.4%	35.7%	338	4563	53
Venice-2	27.0	72.4	3.8%	50.0%	728	5294	46
KITTI-17	17.4	66.8	0.0%	44.4%	23	527	14

VI. COMPLETE OBJECT DETECTION AND TRACKING RESULTS

We show the complete object detection results of the proposed TSSD method on the ImageNet VID validation set in Table VI. At first, SSD is employed as the baseline method. Then, we employ ConvLSTMs following HL-TU and

denote the result as “ConvLSTM”. Subsequently, AC-LSTM is adopted, followed by the result being called “AC-LSTM”. Finally, the result of proposed TSSD including HL-TU, AC-LSTM, and association loss is presented.

Then, the TSSD-OTA’s tracking results for each 2DMOT validation video are shown in Table VII.